PROCEEDINGS OF SCIENCE

Stellar mass black hole candidates in the birthplaces of radio pulsars

Lisa Chmyreva[a,*] **and Grigory M. Beskin**[a,b]

[a] *Special astrophysical observatory of RAS, Nizhny Arkhyz, Russia*

[b] *Kazan (Volga Region) Federal University, Kazan, 420008 Russia*

E-mail: lisa.chmyreva@mail.ru

We performed a search for stellar-mass black hole (BH) candidates in the birth regions of 4 pulsars. We analyzed the available spectral, photometric and astrometric data to isolate 8 objects that exhibit characteristics corresponding to theoretical predictions for isolated BHs. We also discuss the observational manifestations of a stellar mass BH - the recently discovered microlens MOA-2011-BLG-191/OGLE-2011-BLG-0462. The data available for this object are used to calculate the parameters of its local interstellar medium, obtain the accretion rate and luminosity of the object, and construct its theoretical spectrum. A comparison of the spectrum with the sensitivity levels of several instruments shows that direct detection of the emission from this BH is possible for several future observing missions.

The Multifaceted Universe: Theory and Observations - 2022 (MUTO2022)
23-27 May 2022
SAO RAS, Nizhny Arkhyz, Russia

*Speaker

PoS(MUTO2022)057

1. Introduction

A key attribute of black holes (BH) is the presence of an event horizon — a semipermeable membrane that confines the region of space containing the black hole. To identify an object as a BH, one must obtain data from the regions located in direct proximity of the event horizon, which is extremely difficult to do [1]. In X-ray BH binaries, such regions are obscured to a significant degree by the surrounding accreting material. In the case of isolated BHs, the accretion rate is low, allowing one to register photons originating in the immediate vicinity of the event horizon [2]. Isolated BHs are therefore of special interest. They usually undergo spherical accretion [3, 4], and most of the radiation in this case originates at a distance of about 1–2 r_g, where r_g is the gravitational radius.

For typical interstellar medium parameters, and velocities and masses expected for BHs, they would manifest themselves as objects with luminosities ranging from 10^{28} to 10^{34} erg s^{-1}, with continuous spectra lacking lines in a wide frequency range ($10^{14} - 10^{20}$ Hz) [4–7]. Another common property would be light variations with amplitudes ranging from fractions of a percent to ten percent, with the duration of individual flares from 10^{-6} to 10^{-3} s. These objects may also be variable on time scales from months to years. In this work we study objects in regions where the probability of locating a BH is higher: zones of disruption of massive binaries containing BHs and neutron stars (NS), and regions of microlensing events.

2. Determining the probable BH localization regions

With at least 70% of all stars being members of binary and multiple systems, one can assume with a high probability that many of the now single stellar-mass BHs and NSs (pulsars) have also originated in binaries. An analysis of NS (pulsar) kinematics allows one to trace their motion in the past and, using their characteristic age estimates ($\tau_{\rm ch} = P/2\dot{P}$, where P is the pulsar period), determine the probable location of their birth, accompanied by the disruption of such a binary. Assuming that the other companion is a BH, whose mass is several times higher than that of a pulsar, the BH would obtain a smaller velocity after system disruption and, therefore, should be located near the pulsar birthplace. Thus, the *a priori* probability of a BH being located in these regions is enhanced, which allows us to narrow down significantly the search areas for these objects. We used the Monte Carlo method to model a series of pulsar trajectories and determine their location in the epoch corresponding to $\tau_{\rm ch}$. This method is discussed in detail in our paper [8]. The birthplaces of four young pulsars (J 0139+5814, J 0922+0638, J 0358+5413 and J 1935+1616) that have shown good simulation results were used to search for BH candidates.

3. Selection of BH candidates

In the pulsar birth regions described above we selected all gamma, X-ray, and radio sources. Cross identification of these sources within their positional error ellipses lead to 57 matches between X-ray and radio sources. Forty five of these are quasars, stars, or galaxies. Twelve areas were finally selected with sizes of about 10–20″, where the difference between the coordinates of the radio and X-ray sources does not exceed their positional errors. These areas host a total of 35 optical sources. We added 59 white dwarfs and blue objects (with no hard spectral component) to obtain

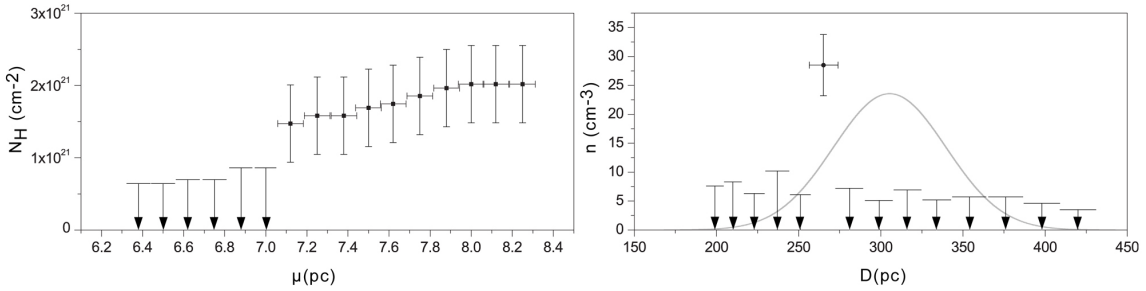

Figure 1: *Left* – sample N_H column density distribution as a function of distance modulus μ for one of the candidates (J 193415.78+190004.2). The errors correspond to the 1σ-level according to the distribution [10]. The upper limits (for a 99% confidence level) are shown by arrows. *Right* – Interstellar medium density n estimate as a function of distance D. The Gaussian shows the distribution of the candidate's distance estimates.

a list of 94 optical objects. From this list, we removed extended sources and artifacts, objects with no proper motions and those with distance estimates outside the determined search locations, objects with spectral lines and objects whose photometric data are well fitted with the Planck curves (regular stars). The final sample consisted of 9 candidates – mainly faint $19^{\rm m}$–$21^{\rm m}$ sources, located at distances up to about 500 pc. Five of the candidates have SDSS photometry available – their colors correspond to the white dwarf and quasar domain.

4. Observed and theoretical properties of the candidates

Based on the classic accretion mechanism concepts [4, 9], the formula for the theoretical luminosity of an isolated BH with spherical accretion, which was used to estimate the luminosities of the nine candidates, can be written as [1]:

$$L = 9.6 \times 10^{33} M_{10}^3 n^2 (V^2 + c_s^2)_{16}^{-3} \ \ \mathrm{erg\ s^{-1}}, \tag{1}$$

where M_{10} is the BH mass in units of $10M_\odot$, n is the medium density in units of $\mathrm{cm^{-3}}$, and V and c_s are the total spatial BH velocity and the sound speed normalized to 16 $\mathrm{km\,s^{-1}}$.

Using standard expressions for luminosity, magnitude and distance modulus, we derive for a BH the relation between mass and velocity. It includes the interstellar medium parameters mentioned above, and the visual magnitude m of an object at distance D_{10} in units of 10 pc:

$$M = 55.44 \times 10^{-(2/15)m} D_{10}^{2/3} n^{-2/3} (V^2 + c_s^2)_{16}. \tag{2}$$

To determine n we used empirical dependences $E_{g-r}(\mu)$ between the reddening E_{g-r} and distance modulus μ for different directions, obtained from the data of the 3D Galactic dust map [10]. Since $N_H = 6.86 \times 10^{21} E_{B-V}$ [11] and $E_{B-V} = 0.884 E_{g-r}$ [10], we have for the hydrogen column density $N_H = f(\mu) = 6.06 \times 10^{21} E_{g-r}(\mu)$. Differentiating this function and taking into account the relation between D and distance modulus $\mu = 5\log(\frac{D}{10})$, we derive the local medium density n in the vicinity of the object:

$$n = \frac{dN_H}{dD} = 6.06 \times 10^{21} \frac{dE_{g-r}(\mu)}{dD(\mu)} = 1.3 \times 10^{21} \times 10^{-\mu/5} \frac{dE_{g-r}(\mu)}{d\mu}. \tag{3}$$

Object	μ''_α, μ''_δ mas yr^{-1}	D pc	$\overline{n}$ cm^{-3}	V_{tr} km s^{-1}	m
J035738.16+525934.4	2.56±0.88, 6.58±0.69	392±70	≤ 4.0	13±3	19.3±0.4
J035757.63+525928.7	-12.5±1.5, 2.6±1.1	377±100	≤ 2.9	23±7	19.6±0.6
J035717.10+511525.4	0.88±0.51, -1.8±0.35	571±70	≤ 2.8	5±1	18.6±0.3
J035239.08+513344.1	18.9±0.5, -26.1±0.4	210±10	7.2±5.4	32±2	18.7±0.1
J193559.98+205305.7	7.4±0.7, 2.7±0.8	466±120	4.8±1.7	17±5	19.7±0.6
J193433.81+203117.1	15.7±0.3, -36.1±0.4	290±20	6.4±3.0	54±4	18.8±0.2
J193415.78+190004.2	0.5±1.2, -41.7±1.7	305±100	3.5±2.4	60±20	20.5±0.8
J034803.12+505358.7	-1.97±1.13, -7.59±0.92	448±200	2.4±1.4	17±8	20.5±1.2
J090946.77–062229.8	5.7±0.9, -21.4±0.8	507±100	≤ 0.9	53±10	18.6±0.5

Table 1: Parameters and their errors for 9 selected candidates. Proper motions μ''_α, μ''_δ, distances D, weighted-average densities $\overline{n}$, transverse velocities $V_{\rm tr}$ and visual magnitudes m are given.

Fig. 1 illustrates this procedure for one sample object (J 193415.78+190004.2). Since the distance uncertainties for the objects are rather large, it is impossible to obtain an exact density value in their vicinity. As an estimate, we used a weighted-average value for the range of acceptable distances, determined by their measurement accuracy. For this estimate, we have $\overline{n} \in (\overline{n}_{\rm min}, \overline{n}_{\rm max})$ with $\overline{n}_{\rm min} = \frac{\sum wn}{\sum w}$ and $\overline{n}_{\rm max} = \frac{\sum wn + \sum wn_0}{\sum w}$, where n are the individual density values, w are their probabilities, and n_0 is the upper density limit estimate.

Since each object has only the transverse component $V_{\rm tr}$ of its total velocity measured, this quantity represents its minimal value and limits the domain of acceptable velocities: $V > V_{\rm tr} = 4.74\mu'' D$, where μ'' is the observed proper motion.

Finally, we estimate the last parameter included in expression (1) — the local sound speed c_s. This quantity was determined using the standard formula $c_s = \sqrt{\frac{\gamma kT}{m_p}}$, where m_p is the proton mass, and the temperature T was estimated from the empirical dependence $T(n)$ [12]. The set of parameters described above is given for each object in Table 1.

To estimate the probability that the candidates are indeed isolated BHs, we used the results of [13] who discuss in detail the evolutionary scenarios for galactic BHs. The standard evolution model for the Galactic disk population yields a two-peak distribution for the velocities and a three-peak mass distribution. Converting these independent distributions to probabilities and multiplying them, we derive a two-dimensional space showing the regions of the most probable M and V values for isolated BHs that originated in binary systems. For each of the 9 candidates, the regions corresponding to their observed and derived parameters were superimposed on this MV plane. The widths of these regions are determined by the accuracies of the quantities in expression (2), i.e. the distance, density, and magnitude errors. Integrating the two-dimensional probability density within the superimposed regions, we derive the total probability P that the candidate is a BH. For clarity, this procedure is illustrated in Fig. 2, which shows the computed regions for the nine candidates combined with the MV plane for isolated stellar-mass BHs.

Out of the nine selected candidates, eight have shown probabilities P ranging from 1.2% to

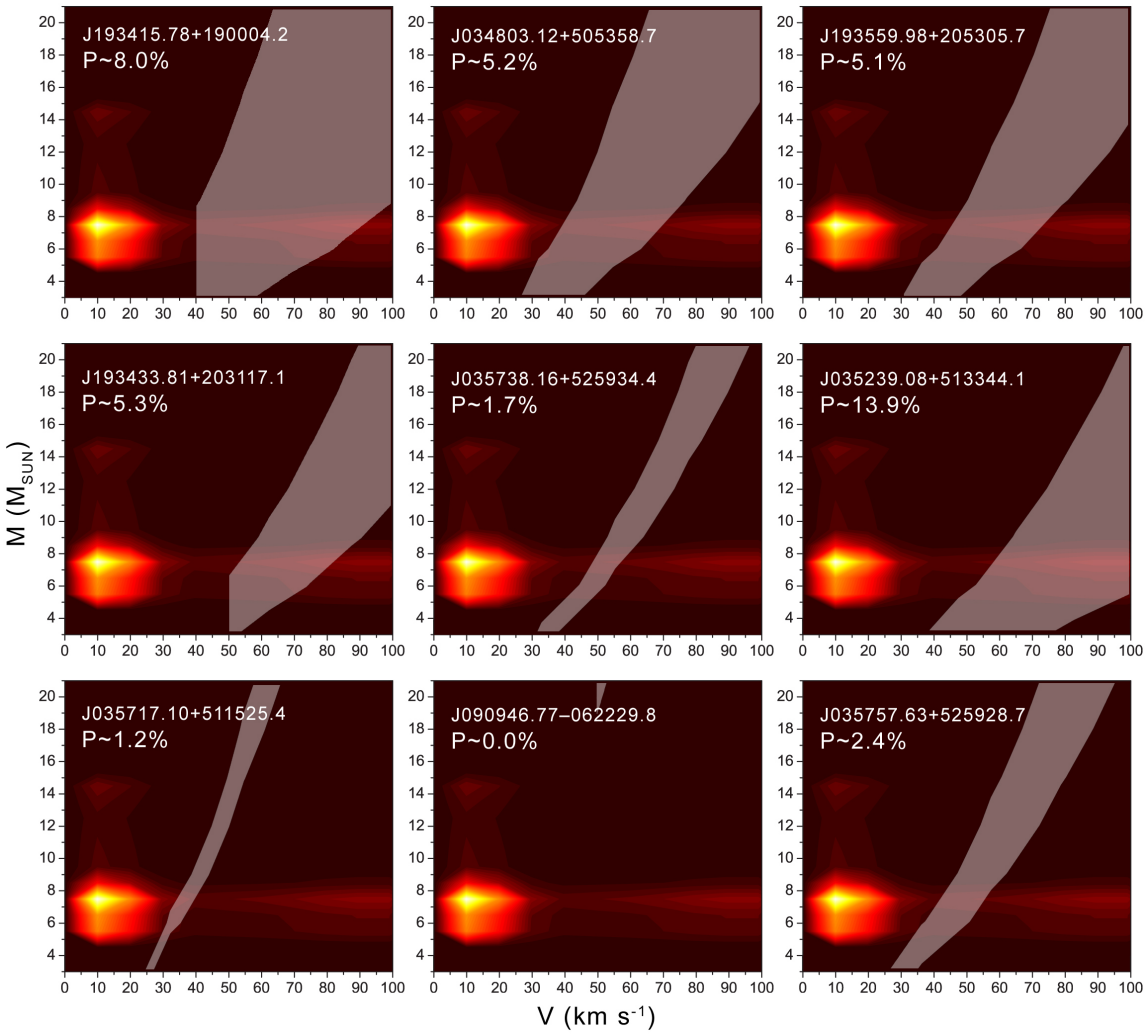

Figure 2: Regions (stripes) of mass M and velocity V values for 9 candidates for which the observed and model parameters are in agreement. The stripes are limited from the left by the minimal velocity estimates corresponding to the observed transverse velocity $V_{\rm tr}$ of each object. The probabilities that the candidates are indeed black holes are given in the top left-hand corner of each panel.

13.9%. One object was excluded from further consideration, since its observed magnitude does not coincide with the theoretical one for any set of parameters. The total probability for the remaining eight candidates to have at least one BH among them is ~ 36% [14].

5. Gravitational lens MOA-11-191/OGLE-11-0462, a probable BH

The only method that allows one to obtain a direct mass estimate for an isolated BH candidate is astrometric microlensing. The gravitational lens MOA-2011-BLG-191/OGLE-2011-BLG-0462 recently discovered by [15] has a mass estimate of $7.1 \pm 1.3\ M_{\odot}$, which leaves no doubt that it is a BH. Since no detectable emission has yet been discovered from this source, we evaluate the capabilities of existing and future astronomical instruments for solving this task. Based on the mass and velocity estimates for the BH and its local interstellar medium parameters, we obtain, within the low rate spherical accretion model, the spectral energy distribution for the emission of matter

accreting onto the lens. Additionally, its stationary (total) and flare components are separated and compared to the sensitivity (existing and planned) of telescopes in different wavelength regions. Our analysis shows that one cannot rule out a possible detection of observational manifestations of the event horizon of MOA-2011-BLG-191/OGLE-2011-BLG-0462.

The magnitudes of the lensed source outside of the brightness increase interval are $m_V = 21.946 \pm 0.014$ and $m_I = 19.581 \pm 0.012$ in the V and I bands, correspondingly [15]. The upper luminosity estimate for the lens is at a level of 1% of the source, i.e. the V-band magnitude of the lens should be fainter than $m_V + 5^m \simeq 27^m$, and thus, with a sufficiently long exposure, the HST may be able to detect the object once it has moved away from the source.

Similar to the computations for the 9 candidates described above, we derive estimates of the medium density, temperature, sound speed in the interstellar medium in the vicinity of the lens. The accretion rate in this case is $\dot{m} = 1.3 \times 10^{-5} M_{10} n (V^2 + c_s^2)_{16}^{-3/2} = 1.19^{+5.35}_{-0.80} \times 10^{-7}$ in Eddington normalization [1], which gives a luminosity of $L = 5.14^{+0.72}_{-0.70} \times 10^{29}$ erg s^{-1}, where V is the difference between the BH and interstellar gas velocities. Taking into account the limiting magnitude, we estimate for the lens a velocity higher than about 60 km s^{-1}. For this value the magnitude limit holds true for approximately the whole range of acceptable medium densities n. The list of parameters for the black hole MOA-11-191/OGLE-11-0462 is presented in Table 2.

Parameter	Value
Coordinates [α, δ (J2000)]	17:51:40.2082, -29:53:26.502
Mass [$M_\odot$]	7.1±1.3
Distance [kpc]	1.58±0.18
Transverse velocity [km s^{-1}]	~45
*Medium density [cm^{-3}]	0.7±0.4
*Temperature [K]	6350±4189
*Sound speed [km s^{-1}]	6.8±3.6
*Luminosity [erg s^{-1}]	$5.14^{+0.72}_{-0.70} \times 10^{29}$
*Accretion rate	$1.19^{+5.35}_{-0.80} \times 10^{-7}$
*Magnitude for $V \gtrsim 60$ km s^{-1}	$\gtrsim 27.87$

Table 2: Parameters of the black hole MOA-11-191/OGLE-11-0462 and their σ level uncertainties. The asterisks mark the quantities obtained in this work

In order to estimate the luminosity of the object in other wavelength ranges we use the results of [1], where spectra were obtained in a wide frequency interval (from radio to gamma) for plasma accreting onto an isolated BH for various properties of both the object and its surrounding medium. Using these computations with the parameters estimated above, we obtain a theoretical spectrum of MOA-11-191/OGLE-11-0462 (presented in Fig. 3), as well as an estimate of the possible flare amplitude (for a given accretion rate its maximum amplitude corresponds to a level of 5.5% of the flux). The object is predictably faint in all spectral regions.

Fig. 3 also compares the sensitivities of the observation instruments in different frequency regions with the derived spectrum of the BH lens. The uncertainties of the velocity, distance,

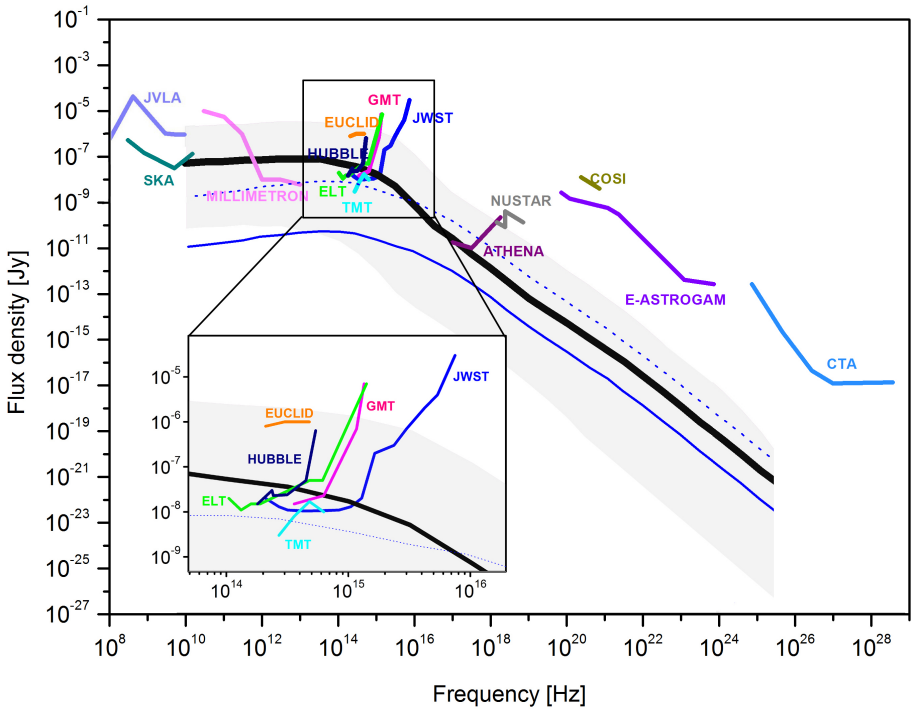

Figure 3: Theoretical spectrum of the black hole MOA-11-191/OGLE-11-0462 with the following parameters: $M = 7.1 \pm 1.3\ M_\odot$, $D = 1.58 \pm 0.18$ kpc, $V_{\rm tr} \sim 45$ km s^{-1}, $n = 0.7 \pm 0.4$ cm^{-3}, $T = 6350 \pm 4189$ K, $c_s = 6.8 \pm 3.6$ km s^{-1}, $L = 5.14^{+0.72}_{-0.70} \times 10^{29}$ erg s^{-1}, $\dot{m} = 1.19^{+5.35}_{-0.80} \times 10^{-7}$. The flux density in Jy is shown as a function of frequency in Hz, the grey area shows the full range of its values corresponding to the acceptable characteristic intervals for the object and interstellar medium. The thick black curve shows the spectrum for $V = 60$ km s^{-1} ($m_V = 27.87$, see text). The maximum amplitude (5.5%) of the possible flares is shown by the thin blue curve, with the dashed curve showing its upper uncertainty. Also shown are the limiting sensitivities of the current and planned observing missions in different frequency ranges. The optical region is emphasized for clarity.

mass and interstellar medium density determine the area of acceptable flux values (grey zone in the figure). Such telescopes as SKA, JVLA, Millimetron, JWST, TMT, GMT, ELT, Athena have sufficient limiting sensitivities for detecting the emission of this object in long exposures (the following exposures are shown in the figure: JWST, HST, ELT, GMT — 10^4 s, ATHENA — 10^5 s, TMT — 1 hour, SKA, CTA — 100 hours, Millimetron — 1 day, e-Astrogam — 1 year). We emphasize that the critical test for registering manifestations of an event horizon is the detection of fast variations in the emission of plasma accreting onto a BH [1, 4]. The typical flare durations are $\tau_v \sim r_g/c \sim 10^{-4}$–$10^{-5}$ s [1], and a temporal resolution of the order of microseconds combined with a high sensitivity of some telescopes will allow the detection of such flares, the shape of which carries information about the properties of space-time near the event horizon. For a detailed discussion see our upcoming paper [16] (*in press*).

6. Conclusions

The presented analysis shows that at least one stellar-mass BH may be present (with a probability of 36%) among the candidate objects located in the birthplaces of the considered pulsars. The black hole MOA-11-191/OGLE-11-0462 with a confirmed mass estimate might be detectable with several upcoming observing missions. The critical test for registering the manifestations of an event horizon is the detection of fast variations in the emission of plasma accreting onto the BH [1, 4]. Establishing

this fact would require observations in two directions. The first is multi-band photometry, which would allow one to determine the character of the continuum for these objects and, in the case of its non-thermal nature, would serve as a serious argument in favor of an accretional origin of their emission. Secondly, observations with a high temporal resolution of up to 10^{-5}–10^{-6} s are needed, which can be used to either detect variations in this range, which are a sign of fragmented accretion onto a BH, or determine the upper limit for the intensity of this emission component.

Acknowledgements

This work was carried out within the framework of the "Fundamental Research" government contract of SAO RAS and the Federal program "Kazan Federal University Competitive Growth Program."

References

[1] G. M. Beskin, et al., *Low-rate accretion onto isolated stellar-mass black holes*, A&A440 (1) (2005) 223–238. arXiv:astro-ph/0403649, doi:10.1051/0004-6361:20040572.

[2] G. Beskin, et al., *Observational appearances of isolated stellar-mass black hole accretion Theory and observations*, Advances in Space Research 42 (3) (2008) 523–532. arXiv:0709.2552, doi:10.1016/j.asr.2007.03.104.

[3] H. Bondi, *On spherically symmetrical accretion*, MNRAS112 (1952) 195. doi:10.1093/mnras/112.2.195.

[4] V. F. Shvartsman, *Halos around "Black Holes"*., Soviet Ast.15 (1971) 377.

[5] Bisnovatyi-Kogan, et al., *The Accretion of Matter by a Collapsing Star in the Presence of a Magnetic Field*, Ap&SS28 (1) (1974) 45–59. doi:10.1007/BF00642237.

[6] P. Meszaros, *Radiation from spherical accretion onto black holes.*, A&A44 (1) (1975) 59–68.

[7] J. R. Ipser, et al., *Synchrotron radiation from spherically accreting black holes*, ApJ255 (1982) 654–673. doi:10.1086/159866.

[8] E. G. Chmyreva, et al., *Search for pairs of isolated radio pulsars—Components in disrupted binary systems*, Astronomy Letters 36 (2) (2010) 116–133. arXiv:1203.2836, doi:10.1134/S1063773710020040.

[9] H. Bondi, et al., *On the mechanism of accretion by stars*, MNRAS104 (1944) 273. doi:10.1093/mnras/104.5.273.

[10] G. M. Green, et al., *A 3D Dust Map Based on Gaia, Pan-STARRS 1, and 2MASS*, ApJ887 (1) (2019) 93. arXiv:1905.02734, doi:10.3847/1538-4357/ab5362.

[11] T. Güver, et al., *The relation between optical extinction and hydrogen column density in the Galaxy*, MNRAS400 (4) (2009) 2050–2053. arXiv:0903.2057, doi:10.1111/j.1365-2966.2009.15598.x.

[12] N. G. Bochkarev, *The interstellar medium and star formation*, 1981, pp. 265–325.

[13] G. Wiktorowicz, et al., *Populations of Stellar-mass Black Holes from Binary Systems*, ApJ885 (1) (2019) 1. arXiv:1907.11431, doi:10.3847/1538-4357/ab45e6.

[14] L. Chmyreva, et al., *Peculiar Objects in the Birthplaces of Radio Pulsars—Stellar-Mass Black Hole Candidates*, Astrophysical Bulletin 77 (1) (2022) 65–77. doi:10.1134/S1990341322010035.

[15] K. C. Sahu, et al., *An Isolated Stellar-Mass Black Hole Detected Through Astrometric Microlensing*, arXiv e-prints (2022) arXiv:2201.13296arXiv:2201.13296.

[16] L. Chmyreva, et al., *On the possibility of direct detection of the emission of microlens MOA-2011-BLG-191/OGLE-2011-BLG-0462—a probable black hole.*, Astrophysical Bulletin 77 (3) (2022) 228–(*in press*).